

Actinide production in reactions of heavy ions with  $^{248}\text{Cm}$ 

Kenton J. Moody,\* Diana Lee, Robert B. Welch,<sup>†</sup> Kenneth E. Gregorich, and Glenn T. Seaborg  
*Nuclear Science Division, Lawrence Berkeley Laboratory,  
 University of California, Berkeley, California 94720*

R. W. Lougheed and E. K. Hulet

*Lawrence Livermore National Laboratory, University of California, Livermore, California 94550*

(Received 19 September 1985)

Transfer reactions of heavy ions with  $^{248}\text{Cm}$  targets are evaluated for their usefulness in producing unknown neutron-rich actinide nuclides. Cross sections for the production of nuclides in the region  $91 \leq Z \leq 100$  were determined radiochemically from bombardments with  $^{18}\text{O}$ ,  $^{86}\text{Kr}$ , and  $^{136}\text{Xe}$  ions. The systematic trends in the cross sections for these reactions can be understood in terms of the Coulomb potential and the stabilizing effect of the reaction  $Q$  values, which tend to favor the production of nuclei with  $Z > Z_{\text{target}}$  with low excitation energies. Extrapolation of the product yields into unknown regions of charge and mass indicates that the use of heavy-ion transfer reactions to produce new neutron-rich above-target species is limited. Substantial production of unknown neutron-rich below-target species is expected in reactions with heavy projectiles like  $^{136}\text{Xe}$  and  $^{238}\text{U}$ .

## I. INTRODUCTION

Recently, there has been a great deal of interest in the use of heavy-ion transfer reactions with actinide targets to produce new nuclear species in the actinide and transactinide regions.<sup>1-7</sup> This work has been focused on reaction products with nuclear charges in excess of that of the target. However, recent successes in synthesizing new near- and below-target species in regions of lower nuclear charge<sup>8,9</sup> have led us to believe there is a possibility of producing new actinide species in similar reactions.

We have performed several experiments in which the actinide products from the interactions of  $^{18}\text{O}$ ,  $^{86}\text{Kr}$ , and  $^{136}\text{Xe}$  with  $^{248}\text{Cm}$  were chemically isolated and their cross sections determined. We use these data, along with literature results from the  $^{48}\text{Ca} + ^{248}\text{Cm}$  system<sup>1,10</sup> and from the  $^{238}\text{U} + ^{248}\text{Cm}$  system,<sup>11</sup> to try to understand the driving force of these reactions, which of the products survive fission, and which reactions are the most useful for producing new, neutron-rich actinide species.

The lack of suitable nuclear reactions to produce new, neutron-rich actinide nuclides has long hindered the study of these nuclides. The undiscovered neutron-rich light actinides are known to be mainly  $\beta^-$  emitters because of the presence, in debris from thermonuclear explosions, of their high  $Z$  daughters, which are thought to arise from a series of rapid, successive neutron captures followed by multiple  $\beta^-$  decays.<sup>12-14</sup> These unknown  $\beta^-$ -decaying nuclides are predicted to have half-lives which are very short compared to the time needed to recover them from the experimental site.<sup>15-17</sup> Therefore, these reactions cannot be used to study these species directly. Complete fusion reactions produce relatively neutron-poor actinide products due to the bend of the valley of beta stability toward neutron excess with increasing proton number. Light-ion stripping and direct reactions with exotic tar-

gets have been used profitably to make new actinide species,<sup>18-21</sup> but these reactions are of little value if the desired neutron-rich product lies outside the immediate mass and charge vicinity of the target nuclide.

The best possibility for producing unknown, neutron-rich actinide nuclides and studying them in the laboratory occurs in heavy-ion transfer reactions with neutron-rich actinide targets. We use the nonspecific term "transfer reaction," since it is probable that actinide reaction products are formed via both partially-damped and quasielastic processes. Transfer reactions proceed via a two-centered intermediate, during whose lifetime mass and charge are exchanged between the participants while kinetic energy and orbital angular momentum are "thermalized" into excitation energy and intrinsic spin. Since there are two outgoing primary products, there is no well-defined final state; the distribution of charge, mass, excitation energy, and angular momentum between the reaction participants provides a finite probability for the formation of neutron-rich, targetlike products with the low excitation energies necessary to survive fission.

In our experiments, we have irradiated targets of  $^{248}\text{Cm}$  with neutron-rich projectiles at energies near and below the nominal Coulomb barrier. The  $^{248}\text{Cm}$  target material was chosen for several reasons: It is a long-lived, neutron-rich actinide nuclide which is available with a high isotopic purity in milligram quantities. Even though it is located near the edge of the known nuclides, there is a wide variety of nearby nuclei with half-lives such that they are observable after off-line chemical separations. In transfer reactions with neutron-rich projectiles, exchanges with  $^{248}\text{Cm}$  yield a range of isotopes of the same element as primary products with nearly the same ground state-to-ground state  $Q$  values (see below).

We have used our experimental results and those of others<sup>5,10,11</sup> to determine from the cross-section systematics

the best reactions for producing new neutron-rich nuclides from  $^{248}\text{Cm}$  targets, and to extend our extrapolations to other targets.

## II. EXPERIMENTAL

Irradiations with  $^{86}\text{Kr}$  ions and  $^{136}\text{Xe}$  ions were performed at the Lawrence Berkeley Laboratory's SuperHILAC. Beams of  $^{86}\text{Kr}$  and  $^{136}\text{Xe}$  with average charge states of  $22^+$  and  $29^+$ , respectively,<sup>22</sup> were delivered to the target system at intensities up to 2 electrical  $\mu\text{A}$ . The target system is described elsewhere.<sup>23,24</sup> The ion beam was collimated to a 6 mm diameter, then passed through a  $1.8\text{ mg/cm}^2$  Havar isolation foil, a volume of nitrogen cooling gas, and the target substrate before reaching the target material. The target used in these experiments was  $2.1\text{ mg/cm}^2$   $^{248}\text{Cm}$  (97% isotopic composition), vacuum evaporated as the fluoride<sup>25</sup> onto a  $2.6\text{ mg/cm}^2$  foil of beryllium metal in a 6.5 mm diameter spot. Recoiling reaction products were collected with truncated conical foils of  $50\text{ mg/cm}^2$  gold or of  $14\text{ mg/cm}^2$  aluminum. These thicknesses were calculated to be more than sufficient to stop products from collisions with full momentum transfer. The residual ion beam passed through a hole in the center of the recoil catcher and stopped in a water-cooled beam dump. The sum of the electrical current deposited in the isolation foil, the target, the recoil catcher foils, and the beam dump was measured with an integrating electrometer, and the integral was recorded periodically to reconstruct the irradiation history. Secondary electrons were magnetically suppressed between the collimator and the isolation foil.

The hole at the center of the conical recoil catcher, which allowed the beam to exit, also allowed reaction products to escape which were emitted at small angles to the beam direction. Reactions of the heavy-ion beams with the recoil-catcher foils would have produced interfering activities requiring additional separations. Assuming a uniform source of recoils 6 mm in diameter and given the catcher foil-target geometry, it can be calculated that all reaction products recoiling at laboratory angles between  $25^\circ$  and  $50^\circ$  to the beam direction were caught by the foil, decreasing to zero at  $0^\circ$  and  $70^\circ$ . The calculated quarter-point angles for targetlike products for the highest energy  $^{86}\text{Kr}$  and  $^{136}\text{Xe}$  irradiations performed for this work are  $43^\circ$  and  $33^\circ$ , respectively,<sup>26</sup> decreasing as the reaction energy decreases. At the energy of the spherical Coulomb barrier, the calculated quarter-point angle reaches  $0^\circ$ . However,  $^{248}\text{Cm}$  is strongly deformed,<sup>27</sup> so the use of a spherical barrier in the calculation is unjustified. Products resulting from the exchange of several nucleons were observed even at "sub-barrier" energies. The formation of these products requires a finite interaction time, implying a shift away from an angular distribution centered at  $0^\circ$ . In calculating cross sections, we assumed that all of the product atoms were collected by the recoil foil. Even with losses at low bombarding energies, we would not expect significant deviations to occur between angular distributions of similar reaction products; thus, the relative values of the cross sections measured in a given experiment are reliable.

The energy lost by very heavy ions in their passage through matter is quite large. As a result, it was important to determine exactly the magnitude of this loss. When the Northcliffe and Schilling range tables<sup>28</sup> were used to calculate the energy lost by 1150 MeV  $^{136}\text{Xe}$  ions in their passage through the isolation foil, the cooling gas, and the target substrate, a value of 220 MeV was obtained. When the tables of Hubert *et al.*<sup>29</sup> were used, a loss of 340 MeV resulted. To resolve this discrepancy, the energy of the beam was measured before and after passing through the target assembly with a Si(Au) surface barrier detector during several of the experiments. Corrections for the pulse-height defect were calculated from literature values.<sup>30</sup> It was found that the measured energy loss agreed to within the accuracy of the measurement ( $\pm 5$  MeV) with that calculated from the range tables of Hubert *et al.* These energy spectra also gave an indication of the amount of energy straggling occurring in the target stack; it was found that the full-width at half-maximum of the energy distribution of the beam leaving the target was much less than the energy loss in the curium layer. Consequently, the upper and lower energy limits given for each experiment are the calculated target entrance and exit energies and do not reflect the smaller contribution from straggling.

A beam of 111 MeV  $^{18}\text{O}^{4+}$  ions from the Lawrence Berkeley Laboratory's 88-inch cyclotron was delivered to a target with intensities up to 3 electrical  $\mu\text{A}$ . The target system has been described in detail previously.<sup>5,24</sup> The target used in these experiments was  $0.5\text{ mg/cm}^2$   $^{248}\text{Cm}$  (97% isotopic composition), electroplated batchwise<sup>31,32</sup> from an isopropanol solution onto a  $2.3\text{ mg/cm}^2$  foil of beryllium metal in a 7 mm diameter spot. As previously described for the SuperHILAC experiments, the collimated beam passed through an isolation foil, cooling gas, and the target substrate before entering the target material. The energy of the beam in the curium deposit was approximately 96 MeV. Recoiling reaction products were collected with planar  $2\text{ mg/cm}^2$  gold foils, through which the beam passed before entering the beam dump. All reaction products recoiling between  $0^\circ$  and  $50^\circ$  to the beam axis encountered the catcher foil. The thickness of the foil was such that it was sufficient to stop the actinide recoil products.<sup>33</sup> In the cross-section calculations, we assumed that all the heavy transfer products were collected by the recoil catchers.

The gold recoil catcher foils were processed using standard chemical procedures,<sup>34-38</sup> as illustrated in Fig. 1. The foil was dissolved in a minimum volume of aqua regia containing tracer nuclides of the elements Pa ( $Z=91$ ) to Am ( $Z=95$ ) in order to obtain chemical yields. The resultant solution was loaded onto anion exchange resin in 9M HCl, which allowed the  $3^+$  actinides ( $Z \geq 95$ ) to pass through, but which adsorbed the light actinides and the gold. The  $3^+$  actinide activities were loaded onto a column of cation exchange resin. The elements Md, Fm, Es, and Cf were sequentially eluted with a pH 3.7 ammonium  $\alpha$ -hydroxyisobutyrate solution. The chemical yield of these samples was  $(75 \pm 5)\%$ , determined from reproducible tests with tracer activities. In irradiations with  $^{18}\text{O}$  ions, the Md, Fm, Es, and Cf fractions were not

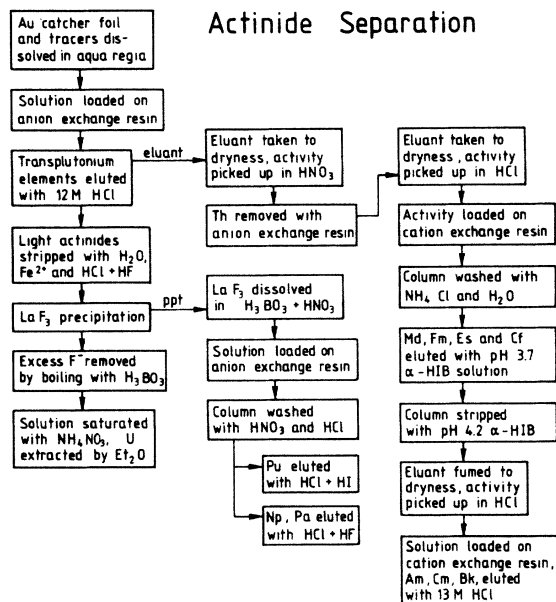


FIG. 1. Chemical procedure used in the separation of the elements from protactinium ( $Z = 91$ ) to mendelevium ( $Z = 101$ ).

generated, since these nuclides have been studied previously in this reaction.<sup>5,6</sup> Am, Cm, and Bk were eluted together from the cation exchange column with a pH 4.2 ammonium  $\alpha$ -hydroxyisobutyrate solution. After destruction of the chelate with  $\text{HNO}_3$  and heat, the activity was loaded onto a column of cation exchange resin in 3M HCl. The actinide elements were eluted with saturated (13M) HCl, leaving the lanthanides behind on the resin. The chemical yield of all three elements was assumed to be equal to that of  $^{241}\text{Am}$  which was introduced as a tracer.

The lighter actinides were eluted from the original anion exchange column with  $\text{Fe}^{2+}$  and dilute solutions of HF and HCl. The elements Pa, Np, and Pu were coprecipitated with lanthanum fluoride. The supernatant liquid was heated with  $\text{H}_3\text{BO}_3$  and then saturated with  $\text{NH}_4\text{NO}_3$ , after which uranium was extracted into diethyl ether. The  $\text{LaF}_3$  precipitate was dissolved in  $\text{H}_3\text{BO}_3$  and  $\text{HNO}_3$  and the solution was loaded onto an anion exchange column. The column was converted to 9M HCl and plutonium was eluted with a solution of HI and HCl. Np and Pa were eluted together with a solution of HCl and HF. Each chemical fraction was prepared for counting by evaporating solutions to dryness on platinum plates which were then ignited.

The above procedure produced samples ready for counting within 2–4 h after the end of irradiation in the  $^{86}\text{Kr}$  and  $^{136}\text{Xe}$  experiments. In the  $^{18}\text{O}$  bombardments, a simplified procedure took 30–60 min, due to the smaller mass of gold and the smaller amounts of background activities. The length of the full procedure required us to perform an extra irradiation during each  $^{86}\text{Kr}$  and  $^{136}\text{Xe}$  experiment to isolate the short-lived neutron-rich americium isotopes. This chemical procedure<sup>39,40</sup> was based on the oxidation of  $\text{Am}^{3+}$  to  $\text{AmO}_2^{2+}$ , which was not coprecipitated with  $\text{LaF}_3$ , followed by reduction and coprecipi-

tation. The americium fractions were prepared as precipitates on nitrocellulose filters within 40 min of the end of the irradiations.

After chemical processing, final samples were counted either for gamma-ray activity or for alpha particle and spontaneous fission decays, depending upon the nuclides of interest. The U, Np/Pa, Pu, Am, and Am/Cm/Bk fractions were counted for gamma rays. The Ge(Li) detector efficiencies were determined for well-defined geometries as a function of gamma-ray energy using a standard source of mixed radionuclides. The resolutions of the detectors were all better than 2.7 keV FWHM for the 1332 keV gamma ray of  $^{60}\text{Co}$ . The gamma-ray spectra of the samples in the energy region of 50 keV to 2 MeV were measured as a function of time after the end of irradiation. In the subsequent data reduction, intensity peaks in these spectra were integrated over a linear background.

The Cf, Es, Fm, and Md fractions were counted for alpha particles and spontaneous fissions. These decays were detected with a set of four Si(Au) surface barrier detectors with active areas of 100 mm<sup>2</sup>. The energy resolution of the counting system was typically 30–40 keV FWHM for the 5.49 MeV alpha particle from  $^{241}\text{Am}$  decay. Spectra were accumulated as a function of time after irradiation. In subsequent data reduction, intensity peaks in these spectra were integrated assuming no detector background, though the contribution from “tailing” of high energy peaks into low energy peaks was subtracted.

Nuclide identifications were made on the basis of both the half-life and the energy of the observed radiation (except for spontaneous fission). Branching ratios and half-lives were taken from the Table of Isotopes,<sup>41</sup> except for those for the decay of  $^{251}\text{Bk}$  (Ref. 42). Cross sections were calculated from the flux history of the bombardments. No corrections were made for “feeding” of one nuclide by another during the relatively long (approximately 12 h) irradiations. This is important only in two of the cases we observed: the  $^{250}\text{Bk}$ - $^{250}\text{Cf}$  pair, where the observed  $^{250}\text{Cf}$  cross section is essentially that of the short-lived  $^{250}\text{Bk}$  parent; and  $^{239}\text{Np}$ , which is fed by  $^{239}\text{U}$  (unobserved).

### III. RESULTS AND DISCUSSION

The cross sections measured in the various experiments are given in Table I, together with the projectile energies entering and leaving the target material. The cross sections vs  $A$  from representative experiments are depicted in Figs. 2–4. In Fig. 4, where the data from our  $^{18}\text{O}$  experiments are plotted with the data from previous experiments, the  $^{250}\text{Cf}$  cross section has been corrected for feeding from  $^{250}\text{Bk}$ . We have found that our berkelium cross sections do not agree with those given in Refs. 5 and 6, ours being larger by a factor of almost 3 for the neutron-rich  $^{250}\text{Bk}$  nuclide.

Figure 5 shows several excitation functions from  $^{86}\text{Kr}$  and  $^{136}\text{Xe}$  reactions with  $^{248}\text{Cm}$ . In the neighborhood of the nominal Coulomb barrier and below, a change in projectile energy does very little to change the relative neutron-richness of the products. Compare, for example,  $^{246}\text{Cf}$  and  $^{254}\text{Cf}$  in the  $^{136}\text{Xe} + ^{248}\text{Cm}$  data, and  $^{246}\text{Cf}$  and

TABLE I. Actinide cross sections from the reaction of heavy ions with  $^{248}\text{Cm}$ .

Ion: Projectile energy in target material (in MeV)	$^{136}\text{Xe}$		$^{86}\text{Kr}$		$^{18}\text{O}^a$				
	Entering Leaving	808 <sup>b</sup> 761	790 699	716 624	546 493	490 436	457 <sup>c</sup> 402	435 379	96.5 95.5
Product	Cross section (in $\mu\text{b}$ )								
$^{232}\text{Pa}$			50±27		75±45				11.4±3.8
$^{234}\text{Pa}^f$		75±30	72±12		30±23				
$^{237}\text{U}$			120±50		240±80				
$^{240}\text{U}$			260±160						
$^{238}\text{Np}$		112±45	116±16	13±11	92±12	56±36	9.5±4.4	≤4	≤4
$^{239}\text{Np}^d$		332±56	227±29	≤22	103±12	76±30	≤20	6.7±3.0	≤7
$^{240}\text{Np}^f$		153±73	125±48						13.6±3.3
$^{243}\text{Pu}$		1100±300	850±180	84±31	680±140	116±33	36±15	15±8	5.3±2.3
$^{245}\text{Pu}$		1430±130	1190±220	92±34	460±80	96±32	26±14	54±31	7.2±3.9
$^{246}\text{Pu}$		1100±150	930±150	79±29	290±40	38±34	23±16	17±10	16.0±8.5
$^{244}\text{Am}^f$			490±40	35.0±5.8	1160±130	167±33	58±11	21±4	65.7±13.6
$^{245}\text{Am}$			2290±440	246±70	3280±680	760±280	300±260	140±47	15±10
$^{246}\text{Am}$ (39 m)			1940±550	180±45	2660±750	650±110	72±25		21±9
$^{246}\text{Am}$ (25 m)			1640±510		2520±810	620±160			72±26
$^{247}\text{Am}$			9960±4180	800±330	8710±4220	2960±690	590±110		20±10
$^{241}\text{Cm}$									9900±700
$^{249}\text{Cm}$			48 000±14 000	10 300±2800	22 500±6400	6000±5500		1430±870	≤8
$^{245}\text{Bk}$			22.1±5.1	1.8±1.6	410±63	41±17	29±9	3.8±1.5	5.1±1.7
$^{246}\text{Bk}$			102±14	6.4±2.3	1400±200	186±41	63±12	22.5±4.3	188±33
$^{248}\text{Bk}^m$			450±130	71±28	3240±500	600±250	220±70	92±32	2860±70
$^{250}\text{Bk}$			1130±80	91±12	2020±200	278±35	107±24	37±6	595±60
$^{251}\text{Bk}$									
$^{246}\text{Cf}$			1.1±0.1	0.036±0.008	28.4±5.3		1.97±0.32	0.48±0.09	
$^{248}\text{Cf}$			93±9	6.1±1.0	790±130		86±14	20.6±3.4	
$^{250}\text{Cf}^d$			980±110	94±14	2620±490		560±90	96±48	
$^{252}\text{Cf}$			138±17	4.7±0.8	142±27		29±13	3.8±0.8	
$^{253}\text{Cf}$			11.6±1.0	0.51±0.09	7.8±1.3		1.25±0.20	0.078±0.017	
$^{254}\text{Cf}$			1.53±0.17	0.026±0.018	0.34±0.07		0.030±0.025		
$^{250}\text{Es}^e$				≤1	104±20		20±14	≤3	
$^{251}\text{Es}$					82±36				
$^{252}\text{Es}$			8.7±1.5	0.212±0.081	53±27		4.0±1.1	0.32±0.08	
$^{253}\text{Es}$			4.4±0.7	0.135±0.026	11.8±1.9		1.6±0.3	0.11±0.02	
$^{254}\text{Es}^m$			1.25±0.14	0.016±0.005	1.25±0.20		0.049±0.011	0.0088±0.0031	
$^{255}\text{Es}$			0.51±0.11	0.015±0.005			0.018±0.006		
$^{256}\text{Es}$ (7.6 h)			0.039±0.009		0.009±0.004				
$^{257}\text{Fm}$			0.084±0.054		5.58±0.80		0.34±0.06	0.082±0.015	
$^{253}\text{Fm}$			0.33±0.12		4.93±1.06		0.52±0.12	0.081±0.020	

TABLE I. (Continued).

Ion: Projectile energy in target material (in MeV)	$^{136}\text{Xe}$		$^{86}\text{Kr}$		$^{18}\text{O}^a$
	Entering Leaving	808 <sup>b</sup> 761	716 624	546 493	435 379
Product	Cross section (in $\mu\text{b}$ )				
$^{254}\text{Fm}$	0.360 $\pm$ 0.075				
$^{255}\text{Fm}$	0.018 $\pm$ 0.009				
$^{256}\text{Fm}$	1.80 $\pm$ 0.31				
	0.205 $\pm$ 0.074				
	<0.015				
	0.069 $\pm$ 0.021				
	0.0186 $\pm$ 0.047				
	0.15 $\pm$ 0.04				
	0.029 $\pm$ 0.008				
	$\leq 0.0025$				

<sup>a</sup>Average results of two experiments performed under the same conditions.

<sup>b</sup>Preliminary experiment performed with a thin target.

<sup>c</sup>Berkelium cross sections are too low in this experiment; losses in the chemical procedure.

<sup>d</sup>Cumulative cross sections.

<sup>e</sup>Sum of both isomeric states; observation via growth of daughter activity.

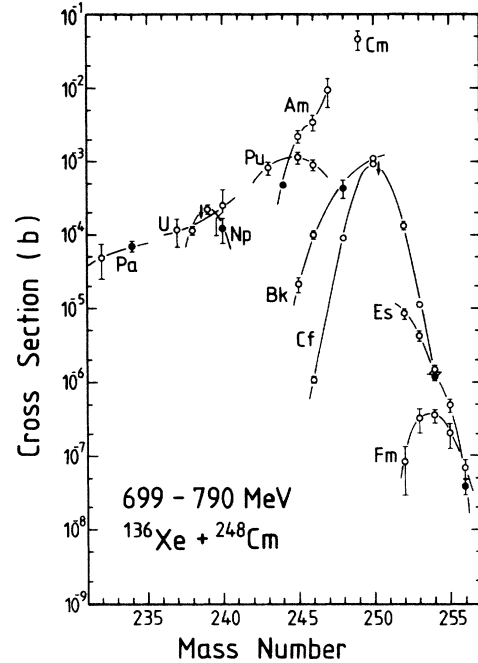


FIG. 2. Actinide yields from the reaction of 699 to 790 MeV  $^{136}\text{Xe}$  ions with  $^{248}\text{Cm}$ . Solid points denote cross sections for single members of isomer pairs.

$^{253}\text{Cf}$  in the  $^{86}\text{Kr} + ^{248}\text{Cm}$  data; near the Coulomb barrier an increase in projectile energy increases the cross sections of neutron-rich and neutron-poor products by a similar amount. In the  $^{86}\text{Kr} + ^{248}\text{Cm}$  system, where a bombardment was performed at a higher energy, 10–20 % in excess of the Coulomb barrier, the neutron-rich products be-

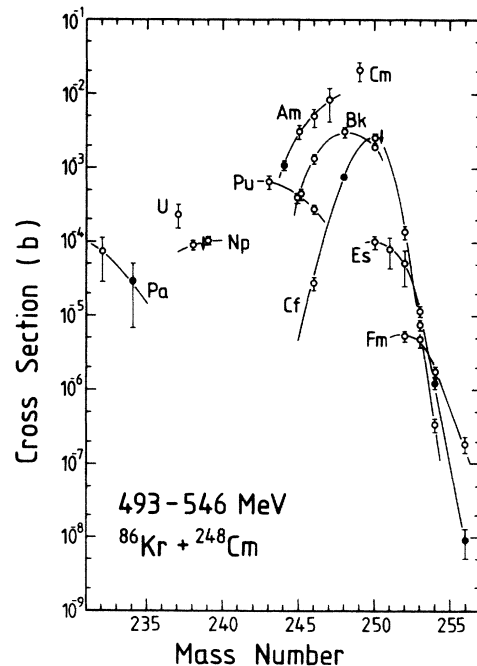


FIG. 3. Actinide yields from the reaction of 493 to 546 MeV  $^{86}\text{Kr}$  ions with  $^{248}\text{Cm}$ . Solid points denote cross sections for single members of isomer pairs.

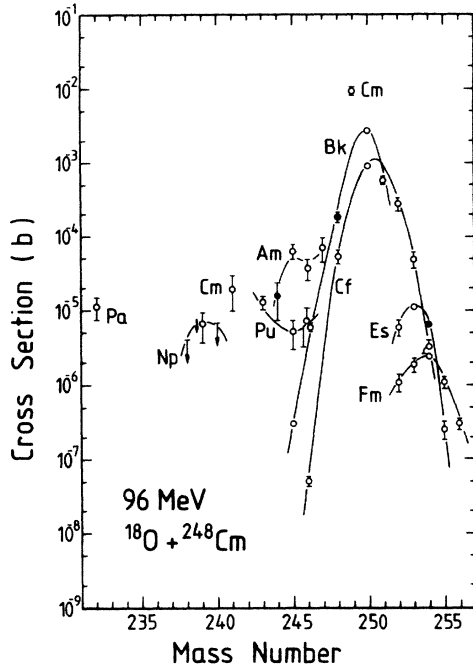


FIG. 4. Actinide yields from the reaction of 95.5 to 96.5 MeV  $^{18}\text{O}$  ions with  $^{248}\text{Cm}$ . Solid points denote cross sections for single members of isomer pairs. Data for  $Z \geq 98$  come from Refs. 5 and 6.

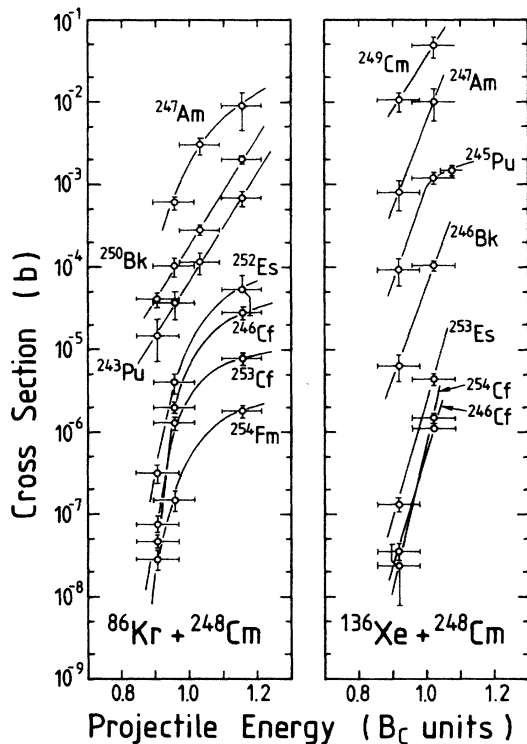


FIG. 5. Some excitation functions from the reactions of  $^{86}\text{Kr}$  and  $^{136}\text{Xe}$  with  $^{248}\text{Cm}$ . The energy is given in terms of a fraction of the nominal Coulomb barrier. Energy error bars describe the difference between the energy of the ions entering and leaving and the target material.

came slightly depleted relative to the neutron-deficient products. At the higher bombarding energy, more excitation energy is thermalized in the reaction, resulting in fractionally more particle emission. The depletion of highly excited products due to fission competition makes the shift away from neutron-richness less important than it would otherwise be. This has also been observed in the  $^{18}\text{O} + ^{248}\text{Cm}$  system<sup>6</sup> where most of the evolved intrinsic energy is deposited in the more massive reaction component. At the energy excesses explored in this work, the cross sections for all surviving evaporation residues are still increasing with energy. At still higher energies, where the mean excitation energy and angular momentum of the primary products is still increasing, the fraction of products which are cool enough to survive fission should decrease more quickly than the slowly-changing reaction cross section increases; therefore the transfer product cross sections should "turn over," starting with those products with the highest ( $Z - Z_{\text{target}}$ ) where the mass flow and excitation energies are largest. This has been observed in  $^{48}\text{Ca} + ^{248}\text{Cm}$  bombardments at several energies up to 20% in excess of the Coulomb barrier<sup>10,43</sup> and in  $^{18}\text{O} + ^{248}\text{Cm}$  bombardments.<sup>6</sup>

A measure of the angular momentum in products surviving fission can be obtained from isomer ratios.<sup>44-46</sup> In  $^{246}\text{Am}$  the two isomers have roughly the same mass excess; the 25-min isomer has  $J^\pi = 2^-$  and the 39-min isomer has  $J^\pi = 7^-$  (Ref. 41). If the mean intrinsic angular momentum of the primary products which survive fission to result in  $^{246}\text{Am}^{m,g}$  was significantly greater than  $7\hbar$ , production of the 39-min isomer would dominate. Instead, the two isomers were produced in roughly equal amounts in all of our experiments, though the data are poor in the case of the  $^{18}\text{O} + ^{248}\text{Cm}$  reaction. The primary products which deexcite to produce  $^{254}\text{Es}^{m,g}$  should have higher intrinsic angular momenta than those which produce  $^{246}\text{Am}^{m,g}$ , since the reaction producing  $^{254}\text{Es}$  (g.s.  $J^\pi = 7^+$ ) involves the exchange of a larger number of nucleons. Yet the observed  $^{254}\text{Es}^m$  ( $J^\pi = 2^+$ ) seems to result from the deexcitation of primary products with little more angular momentum than those producing  $^{246}\text{Am}^{m,g}$ . Very high angular momentum components in the primary distributions are severely depleted by fission.<sup>47</sup>

A striking difference between the reaction of very heavy ions like  $^{86}\text{Kr}$  and  $^{136}\text{Xe}$  and the reaction of light heavy ions like  $^{18}\text{O}$  with  $^{248}\text{Cm}$  is the apparent augmentation of above-target products and the depletion of below-target products in the light heavy-ion reactions. This is due primarily to the combination of two components of the potential energy governing the nucleon exchange: the reaction  $Q$  values and the Coulomb separation energies. In Fig. 6, the Coulomb potentials of touching spheres arising from the binary reactions indicated, assuming a uniform charge density (UCD) in the reacting system and a touching sphere radius as defined by Lefort,<sup>48</sup> are plotted as a function of the  $Z$  of the heavy primary product. The Coulomb potentials of the initial systems have been subtracted. From a purely Coulomb viewpoint, the removal of protons from the target to the projectile is unfavorable, and in the case of  $^{18}\text{O}$  reactions, where the exchange of even one proton is a substantial fraction of the whole pro-

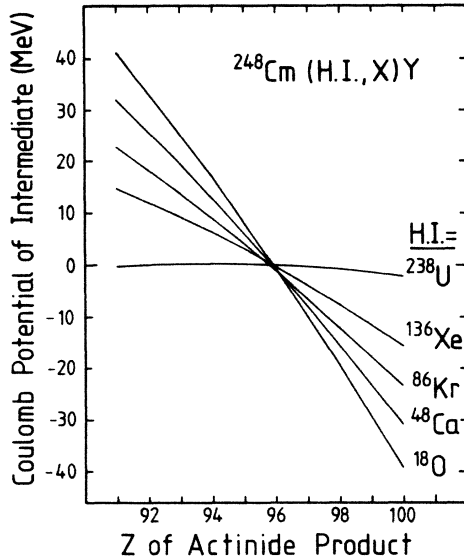


FIG. 6. The difference between the Coulomb repulsive energy of two touching spherical reaction products and the Coulomb energy of the reactants at contact. The equilibrium  $N/Z$  from a uniform charge density assumption is used in calculating the hard sphere radii of the separating systems. The Coulomb driving force of the reactions is toward asymmetry.

jectile, it is particularly unfavorable. In the intermediate colliding system, the tendency will be for protons to flow toward the large fragment.

Figure 7 shows the ground state-to-ground state  $Q$  values for forming representative nuclides from  $^{248}\text{Cm}$  in binary reactions with various heavy ions.<sup>27,41</sup> Once again, the most striking results are obtained in reactions with the lightest ions. The production of fermium isotopes in the reaction of  $^{18}\text{O}$  ions with  $^{248}\text{Cm}$  is "endothermic" by 30–50 MeV. In the reaction of  $^{136}\text{Xe}$  with  $^{248}\text{Cm}$ , the production of fermium nuclides is endothermic by only about 20 MeV. This negative  $Q$  value acts to decrease the

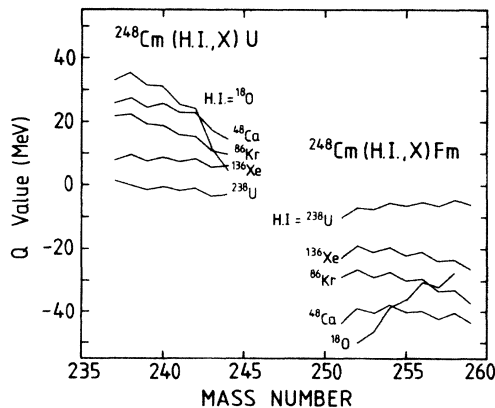


FIG. 7. Ground state-to-ground state  $Q$  values for formation of representative actinide reaction products arising from several heavy ion reactions with  $^{248}\text{Cm}$  targets. Production of below-target nuclides is exothermic. The mass excess data used in the calculations were taken from Refs. 27 and 41.

excitation energy of the primary fermium products, allowing more to survive fission. Not only is the production of below-target species unfavorable from the Coulomb energetics, but those products which are formed are depleted by fission deexcitation due to the "exothermic" nature of the reaction. However, some of the  $Q$ -value advantage of the lighter systems is compensated by the difference in energy between the entrance- and exit-channel Coulomb potentials.

Our data have shown that the neutron-richness of the reaction products is only weakly dependent upon the projectile energy near the Coulomb barrier. The average number of neutrons emitted in the deexcitation of the primary products is determined by a combination of the height of the fission barrier and the population of states near the lower edge of the excitation-energy distributions at low angular momentum. The population of additional states at higher excitation energy in a fermium nuclide will not directly increase the number of neutrons that have to be emitted to deexcite the primary product; rather, it decreases the fractional number of primary products which survive the fission process. Figure 8 shows the fermium isotope cross sections from several experiments, all performed with projectile energies in the neighborhood of, or slightly over, the nominal Coulomb barrier, plotted against the difference between the isotope mass and the mass of a  $Z=100$  species with the  $N/Z$  of the composite intermediate of the reaction (uniform charge density). The formation of fermium isotopes occurs via a sufficiently large exchange between  $^{248}\text{Cm}$  and the projectile that it can be thought of as being due to a damped reaction not having any peripheral, quasielastic contributions.

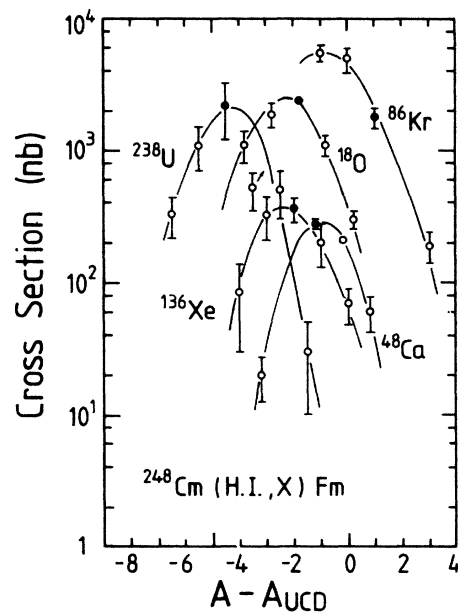


FIG. 8. Production of fermium isotopes from several heavy ion reactions with  $^{248}\text{Cm}$  at energies near the nominal Coulomb barrier. The data are plotted against the difference of the nuclide mass number and the mass expected for a  $Z=100$  species arising from a uniform charge density intermediate. The  $^{254}\text{Fm}$  data points are filled in.

The peaks in the fermium cross section distributions from  $^{48}\text{Ca}$  (Ref. 10) and  $^{86}\text{Kr}$  reactions with  $^{248}\text{Cm}$  are about one mass number below the peak expected for the primary products. As the mass of the projectile increases, the deviation between the observed peak and the calculated peak increases. In bombardments with  $^{136}\text{Xe}$ , the peak in the fermium cross section distribution is about 2.5 mass units below the uniform charge density value, and in bombardments with  $^{238}\text{U}$  ions (Ref. 11) the peak is about four mass units below the calculation. Since the  $Q$  values for making the fermium isotopes are roughly constant (Fig. 7) in all four of these reacting systems, and since the relative fission width is only slowly varying across the limited range of the fermium nuclides under discussion,<sup>49,50</sup> we attribute the deviation between the observed peaks and the calculated peaks to neutron emission. The numbers we obtain for the average number of neutrons emitted in the  $^{48}\text{Ca} + ^{248}\text{Cm}$  system (one neutron), the  $^{136}\text{Xe} + ^{248}\text{Cm}$  system (2.5 neutrons), and the  $^{238}\text{U} + ^{248}\text{Cm}$  system (four neutrons) are in close agreement with those obtained from more elaborate calculations based on experimentally justified  $\Gamma_n/\Gamma_f$  values.<sup>11</sup> We attribute the disagreement between our result of an apparent emission of two neutrons in the  $^{18}\text{O} + ^{248}\text{Cm}$  system and the calculated value of one emitted neutron in Ref. 11 to the effect of rapidly changing  $Q$  values (Fig. 7). When we performed a full potential energy minimization calculation<sup>51</sup> on the  $^{18}\text{O} + ^{248}\text{Cm}$  system, we obtained a most probable fermium mass less than that arising from our UCD assumption.

Even though the primary products of damped collisions of the heaviest ions with  $^{248}\text{Cm}$  lose more neutrons in their deexcitation than the primary products formed in reactions of lighter ions with  $^{248}\text{Cm}$ , the absolute neutron-richness of the final products is roughly the same in both cases due to the relative neutron-richness of the reacting systems. The  $^{254}\text{Fm}$  nuclide is designated by a solid point in each distribution in Fig. 8. This shows that the position of the peak in the fermium cross sections is located at roughly the same mass number in each reaction except for the  $^{86}\text{Kr} + ^{248}\text{Cm}$  system, which has a lower  $N/Z$  (1.530) than any of the other composite systems (from 1.552 for  $^{48}\text{Ca} + ^{248}\text{Cm}$  to 1.585 for  $^{238}\text{U} + ^{248}\text{Cm}$ ). The projectile which is capable of producing new, neutron-rich actinides with the largest cross sections in damped collisions is, then, the one which produces the broadest cross-section distribution in the element of interest. This is expected to be the largest projectile, not only due to the enhanced statistical fluctuation of neutrons and protons in the separating system, but also due to small contributions of products formed in deexcitation channels involving the emission of significantly fewer neutrons than those resulting in the peaks of the isotopic distributions. This is demonstrated in Fig. 9, where the cross sections of the heaviest californium isotopes (produced in the same experiments that gave the data in Fig. 8) are plotted against mass number. Clearly, the  $^{136}\text{Xe}$  and  $^{238}\text{U}$  projectiles are superior to the lighter ions for production of californium isotopes heavier than mass 255.

Figure 10 shows the excitation functions for the production of the isobaric species  $^{253}\text{Es}$  and  $^{253}\text{Cf}$  produced in the reactions of heavy ions with  $^{248}\text{Cm}$ . Production of

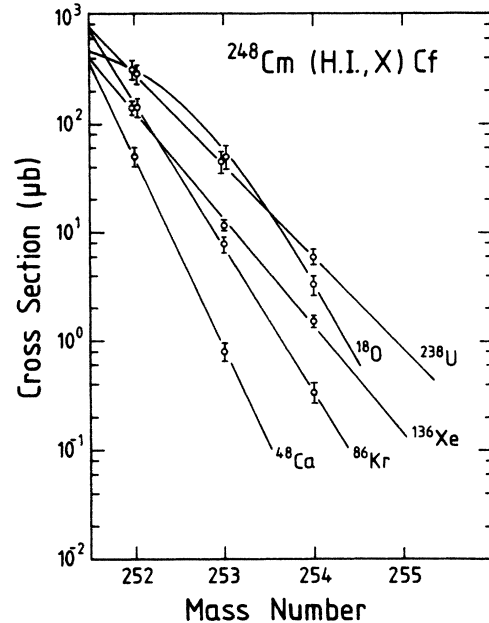


FIG. 9. Neutron-rich californium yields arising from the reaction of various heavy ions with  $^{248}\text{Cm}$ .

$^{253}\text{Es}$  is best accomplished with the light projectile  $^{18}\text{O}$ . A single curve can be drawn through the  $^{253}\text{Es}$  cross sections arising from  $^{86}\text{Kr}$ ,  $^{136}\text{Xe}$ , and  $^{238}\text{U}$  bombardments. For the more neutron-rich  $^{253}\text{Cf}$ , the cross sections from  $^{48}\text{Ca}$  and  $^{86}\text{Kr}$  bombardments are well below those from  $^{136}\text{Xe}$  and  $^{238}\text{U}$  bombardments (connected with a single curve), and the data from  $^{18}\text{O}$  bombardments look relatively less favorable. Extrapolating along the isobar, we conclude that  $^{136}\text{Xe}$  and  $^{238}\text{U}$  projectiles will produce the most  $^{253}\text{Bk}$  in reactions with  $^{248}\text{Cm}$  targets.

Examination of the chart of the nuclides shows that, with neutron-rich actinide targets, considerable transfer of mass has to take place to reach unknown neutron-rich nuclides at a higher  $Z$  than that of the target. However,

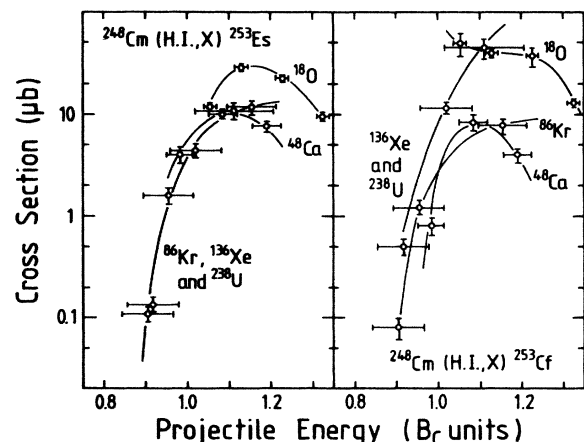


FIG. 10. The production of  $^{253}\text{Es}$  and  $^{253}\text{Cf}$  from the reaction of heavy ions with  $^{248}\text{Cm}$  as a function of energy relative to the Coulomb barrier.



most of these target nuclides have charge and mass values very near those of the last known nuclei with  $Z < Z_{\text{target}}$ . While a damped mechanism must be assumed for the formation of new, above-target nuclides in these transfer reactions, below-target nuclides can be produced in more peripheral reactions. This offers two advantages: Not only are the intrinsic energies and angular momenta of the primary products lower, but the neutron-richness of the actinide products is determined more by the neutron number of the target than by the  $N/Z$  of the composite system. Figure 11 shows a comparison of the excitation functions of  $^{243}\text{Pu}$  and  $^{246}\text{Pu}$  produced in reactions of various heavy ions with  $^{248}\text{Cm}$ . The augmentation of  $^{246}\text{Pu}$  yields is seen in the  $^{136}\text{Xe} + ^{248}\text{Cm}$  system relative to the other reactions with lighter projectiles. This is due in part to the more exothermic nature of the reactions with lighter projectiles and an increase in particle evaporation in the deexcitation of the primary products, and in part to the neutron-richness of the  $^{136}\text{Xe}$  projectile ( $N/Z = 1.52$ , relative to 1.39 for  $^{86}\text{Kr}$  and 1.4 for  $^{48}\text{Ca}$ ). We are optimistic about the possibility of producing new actinide nuclides with  $Z < Z_{\text{target}}$  in reactions of heavy ions with  $^{248}\text{Cm}$ . With heavy projectiles like  $^{136}\text{Xe}$  and  $^{238}\text{U}$ , in bombardments of  $^{248}\text{Cm}$  at energies 10% in excess of the Coulomb barrier, the production of the  $\beta^-$ -emitting nuclides  $^{248}\text{Am}$ ,  $^{249}\text{Am}$ , and  $^{247}\text{Pu}$  should take place with cross sections on the 0.1–1 mb level.

Extrapolations of cross-section distributions for particular elements produced in the reactions of heavy ions with  $^{248}\text{Cm}$  indicate that the synthesis of neutron-rich new nuclides with  $Z > Z_{\text{target}}$  occurs with only very low yield. Cross sections of 10 nb or less can be expected for the production of  $\beta^-$ -decaying  $^{257}\text{Cf}$  and  $^{257}\text{Es}$  in reactions of  $^{136}\text{Xe}$  or  $^{238}\text{U}$  with  $^{248}\text{Cm}$  at an energy in excess of the nominal Coulomb barrier by roughly 10%. The cross section for  $^{260}\text{Fm}$ , which is probably a very short-lived spontaneous fission activity, should be on the order of 100 pb in the same reactions. The production of  $\beta^-$ -decaying  $^{252}\text{Bk}$  is expected to take place with a cross section on the order of 10–100  $\mu\text{b}$ , making it the only unknown above-target nuclide which could be observed in experiments utilizing transfer reactions with  $^{248}\text{Cm}$  targets.

In irradiations of heavy actinide targets with  $^{18}\text{O}$  ions,<sup>4,6</sup> the production of nuclides in transfer reactions with a given number of neutrons and protons more than the target nuclide proceed with cross sections which are only weakly dependent upon the identity of the target. By assuming that this holds true for all projectiles, we have extended our extrapolations to different projectile-target combinations. We conclude that the use of heavy-ion transfer reactions to produce unknown neutron-rich nuclei with atomic numbers higher than that of the target is limited. Only  $^{254}\text{Es}$  lies in a region permitting the production of new above-target activities in significant amounts.<sup>4</sup> However, unknown below-target nuclide production of elements between actinium ( $Z = 89$ ) and berkelium ( $Z = 97$ ) should be possible using target materials like  $^{238}\text{U}$ ,  $^{244}\text{Pu}$ ,  $^{248}\text{Cm}$ , and  $^{252}\text{Cf}$  and heavy ions such as  $^{136}\text{Xe}$  and  $^{238}\text{U}$  at energies near the nominal Coulomb barrier.

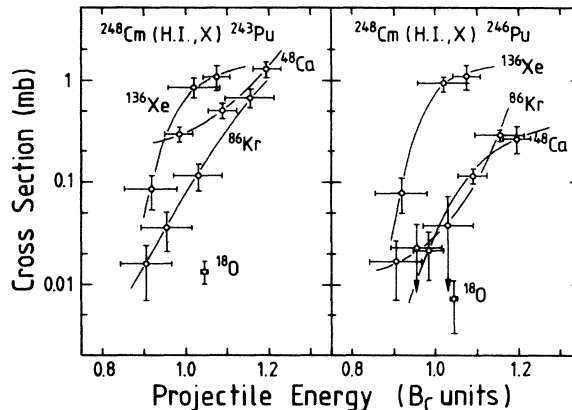


FIG. 11. The production of  $^{243}\text{Pu}$  and  $^{246}\text{Pu}$  from the reaction of heavy ions with  $^{248}\text{Cm}$  as a function of energy relative to the Coulomb barrier.

#### IV. CONCLUSIONS

The production of neutron-rich actinide nuclides in heavy-ion transfer reactions with actinide targets can be understood in terms of the opposing effects of the reaction  $Q$  values and the Coulomb potential of the reaction intermediate. Near the nominal Coulomb barrier, changes in the reaction energy have little effect on the neutron-richness of the products due to the competition of fission with neutron emission at high excitation energies. Only primary products with relatively low angular momenta contribute significantly to the cross sections of the observed activities.

The use of heavy-ion transfer reactions to produce new, neutron-rich above-target nuclides is limited; however, in reactions of very heavy ions with neutron-rich targets like  $^{244}\text{Pu}$ ,  $^{248}\text{Cm}$ , and  $^{252}\text{Cf}$ , significant production of new below-target species is expected.

#### ACKNOWLEDGMENTS

We would like to thank the staffs and crews of the SuperHILAC and the 88-inch cyclotron for their assistance and support. M. Nurmi and A. Ghiorso are gratefully acknowledged for their help with the experiments. We would also like to thank D. C. Hoffman, H. R. von Gunten, P. A. Baisden, K. E. Thomas, and M. Schädel for useful suggestions and discussions. The authors are indebted for the use of the target material to the Office of Basic Energy Sciences, U.S. Department of Energy, through the transplutonium element production facilities at the Oak Ridge National Laboratory. This work was supported by the Director, Office of Energy Research, Division of Nuclear Physics of the Office of High Energy and Nuclear Physics of the U.S. Department of Energy under contract No. DE-AC03-76SF00098.

- \*Present address: L-232, Lawrence Livermore National Laboratory, Livermore, CA 94550.
- †Present address: Universität Bern, CH-3012 Bern-9, Switzerland.
- 1E. Hulet, R. Loughheed, J. Wild, J. Landrum, P. Stevenson, A. Ghiorso, J. Nitschke, R. Otto, D. Morrissey, P. Baisden, B. Gavin, D. Lee, R. Silva, M. Fowler, and G. Seaborg, *Phys. Rev. Lett.* **39**, 385 (1977).
  - 2M. Schädel, J. Kratz, H. Ahrens, W. Bröchle, G. Franz, H. Gäggeler, I. Warnecke, G. Wirth, G. Herrmann, N. Trautmann, and M. Weis, *Phys. Rev. Lett.* **41**, 469 (1978).
  - 3K. Thomas, Lawrence Berkeley Laboratory Report LBL-9886, 1979.
  - 4M. Schädel, W. Bröchle, M. Brügger, H. Gäggeler, K. Moody, D. Schardt, K. Sümmerer, E. Hulet, A. Dougan, R. Dougan, J. Landrum, R. Loughheed, J. Wild, and G. O'Kelley, submitted to *Phys. Rev. C*.
  - 5D. Lee, H. von Gunten, B. Jacak, M. Nurmi, Y.-F. Liu, C. Luo, G. Seaborg, and D. Hoffman, *Phys. Rev. C* **25**, 286 (1982).
  - 6D. Lee, K. Moody, M. Nurmi, G. Seaborg, H. von Gunten, and D. Hoffman, *Phys. Rev. C* **27**, 2656 (1983).
  - 7L. Somerville, Lawrence Berkeley Laboratory Report LBL-14050, 1982.
  - 8R. Kirchner, O. Klepper, W. Kurcewicz, E. Roeckl, E. Zganjar, E. Runte, W.-D. Schmidt-Ott, P. Tidemand-Petersson, N. Kaffrell, P. Peuser, and K. Rykaczewski, *Nucl. Phys. A* **378**, 549 (1982).
  - 9K. Rykaczewski, R. Kirchner, W. Kurcewicz, D. Schardt, N. Kaffrell, P. Peuser, E. Runte, W.-D. Schmidt-Ott, P. Tidemand-Petersson, and K.-L. Gippert, *Z. Phys. A* **309**, 273 (1983).
  - 10D. Hoffman, M. Fowler, W. Daniels, H. von Gunten, D. Lee, K. Moody, K. Gregorich, R. Welch, G. Seaborg, W. Bröchle, M. Brügger, H. Gäggeler, M. Schädel, K. Sümmerer, G. Wirth, T. Blaich, G. Herrmann, N. Hildebrand, J. Kratz, M. Lerch, and N. Trautmann, *Phys. Rev. C* **31**, 1763 (1985).
  - 11M. Schädel, W. Bröchle, H. Gäggeler, J. Kratz, K. Sümmerer, G. Wirth, G. Herrmann, R. Stakemann, G. Tittel, N. Trautmann, J. Nitschke, E. Hulet, R. Loughheed, R. Hahn, and R. Ferguson, *Phys. Rev. Lett.* **48**, 852 (1982).
  - 12Combined Radiochemistry Group, *Phys. Rev.* **148**, 1192 (1966).
  - 13P. Fields, M. Studier, H. Diamond, J. Mech, M. Inghram, G. Pyle, C. Stevens, S. Fried, W. Manning, A. Ghiorso, S. Thompson, G. Higgins, and G. Seaborg, *Phys. Rev.* **102**, 180 (1956).
  - 14H. Meldner, G. Cowan, J. Nix, and R. Stoughton, *Phys. Rev. C* **13**, 182 (1976).
  - 15N. Kolesnikov and A. Demin, Joint Institute for Nuclear Research Report JINR P6-9421, 1975.
  - 16K. Takahashi, M. Yamada, and T. Kondoh, *At. Data Nucl. Data Tables* **12**, 101 (1973).
  - 17H. Klapdor, J. Metzinger, and T. Oda, *At. Data Nucl. Data Tables* **31**, 81 (1984).
  - 18D. Hoffman, J. Wilhelmy, J. Weber, W. Daniels, E. Hulet, R. Loughheed, J. Landrum, J. Wild, and R. Dupzyk, *Phys. Rev. C* **21**, 972 (1980).
  - 19E. Hulet, R. Loughheed, J. Landrum, J. Wild, D. Hoffman, J. Weber, and J. Wilhelmy, *Phys. Rev. C* **21**, 966 (1980).
  - 20P. Hausteiner, H.-C. Hseuh, R. Klobucher, E.-M. Franz, S. Katcoff, and L. Peker, *Phys. Rev. C* **19**, 2332 (1979).
  - 21C. Orth, W. Daniels, and B. Dropesky, *Phys. Rev. C* **8**, 2364 (1973).
  - 22SuperHILAC User's Manual, Lawrence Berkeley Laboratory, Publication 102, 1979.
  - 23K. Moody, M. Nurmi, and G. Seaborg, Annual Report of the Nuclear Science Division, Lawrence Berkeley Laboratory Report LBL-11588, 1981, p. 188.
  - 24K. Moody, Lawrence Berkeley Laboratory Report LBL-16249, 1983.
  - 25R. Loughheed and E. Hulet, *Nucl. Instrum. Methods* **166**, 329 (1979).
  - 26W. Wilcke, J. Birkelund, H. Wollersheim, A. Hoover, J. Huizenga, W. Schröder, and L. Tubbs, *At. Data Nucl. Data Tables* **25**, 389 (1980).
  - 27W. Myers, *Droplet Model of Atomic Nuclei* (IFI/Plenum, New York, 1977).
  - 28L. Northcliffe and R. Schilling, *Nucl. Data Tables A7*, 233 (1970).
  - 29F. Hubert, A. Fleury, R. Bimbot, and D. Gardes, *Ann. Phys. (Paris)* **5**, 1 (1980).
  - 30J. Moulton, J. Stevenson, R. Schmitt, and G. Wozniak, *Nucl. Instrum. Methods* **157**, 325 (1978).
  - 31D. Aumann and G. Müllen, *Nucl. Instrum. Methods* **115**, 75 (1974).
  - 32G. Müllen and D. Aumann, *Nucl. Instrum. Methods* **128**, 425 (1975).
  - 33R. McFarland, Lawrence Berkeley Laboratory Report LBL-15027, 1982.
  - 34R. Penneman and T. Keenan, National Academy of Science-National Research Council Report NAS-NS-3006, 1960.
  - 35J. Grindler, National Academy of Science-National Research Council Report NAS-NS-3050, 1962.
  - 36G. Burney and R. Harbour, National Academy of Science-National Research Council Report NAS-NS-3060, 1974.
  - 37G. Coleman, National Academy of Science-National Research Council Report NAS-NS-3058, 1965.
  - 38G. Higgins, National Academy of Science-National Research Council Report NAS-NS-3031, 1960.
  - 39F. Moore, *Anal. Chem.* **35**, 715 (1963).
  - 40H. Holcomb, *Anal. Chem.* **36**, 2329 (1964).
  - 41*Table of Isotopes*, 7th ed., edited by C. Lederer and V. Shirley (Wiley, New York, 1978).
  - 42Y.-F. Liu, K. Moody, D. Lee, Y. Morita, G. Seaborg, and H. von Gunten, *Nucl. Phys. A* **417**, 365 (1984).
  - 43H. Gäggeler, W. Bröchle, M. Brügger, M. Schädel, K. Sümmerer, G. Wirth, A. Ghiorso, K. Gregorich, D. Lee, K. Moody, G. Seaborg, R. Welch, P. Wilmarth, G. Herrmann, J. Kratz, N. Trautmann, N. Hildebrand, U. Hickmann, C. Frink, N. Greulich, D. Hoffman, M. Fowler, and H. von Gunten, Gesellschaft für Schwerionenforschung Report GSI-83-9, 1983.
  - 44H. Groening, K. Aleklett, K. Moody, P. McGaughey, W. Loveland, and G. Seaborg, *Nucl. Phys. A* **389**, 80 (1982).
  - 45H. Groening, K. Moody, and G. Seaborg, *Nucl. Instrum. Methods* **214**, 317 (1983).
  - 46S. Tanaka, K. Moody, and G. Seaborg, *Phys. Rev. C* **30**, 911 (1984).
  - 47M. Blann and T. Komoto, *Phys. Rev. C* **26**, 472 (1982).
  - 48M. Lefort, *Rep. Prog. Phys.* **39**, 129 (1976).
  - 49T. Sikkeland, A. Ghiorso, and M. Nurmi, *Phys. Rev.* **172**, 1232 (1968).
  - 50H. Gäggeler, A. Iljinov, G. Popeko, W. Seidel, G. Ter-Akopian, and S. Tretyakova, *Z. Phys. A* **289**, 415 (1979).
  - 51R. B. Welch, Lawrence Berkeley Laboratory Report LBL-19010, 1985.